

UNCLASSIFIED

Defense Technical Information Center  
Compilation Part Notice

ADP012511

TITLE: Dusty Plasmas under Microgravity

DISTRIBUTION: Approved for public release, distribution unlimited

This paper is part of the following report:

TITLE: Non-Neutral Plasma Physics 4. Workshop on Non-Neutral Plasmas  
[2001] Held in San Diego, California on 30 July-2 August 2001

To order the complete compilation report, use: ADA404831

The component part is provided here to allow users access to individually authored sections of proceedings, annals, symposia, etc. However, the component should be considered within the context of the overall compilation report and not as a stand-alone technical report.

The following component part numbers comprise the compilation report:

ADP012489 thru ADP012577

UNCLASSIFIED

# Dusty Plasmas under Microgravity

Hiroo Totsuji, Chieko Totsuji, Tokunari Kishimoto and Kenji Tsuruta

*Graduate School of Natural Science and Technology and Faculty of Engineering,  
Okayama University, Tsushimanaka 3-1-1, Okayama 700-8530, Japan*

**Abstract.** The structures of Yukawa systems spherically confined under the condition of microgravity are analyzed by molecular dynamics simulations. It is shown that the system is separated into the outer and the inner parts and well-developed shells appear in the outer part at low temperatures. In the case of Yukawa mixtures, there occurs the separation of species according to the magnitude of charges.

## INTRODUCTION

Dusty plasmas have provided us with an important example of nonneutral plasmas. One of main differences from other nonneutral plasmas composed of ions or electrons is that dust particles have large masses and the effect of gravity plays a key role in determining their behavior.

Recently, some experiments under the condition of the microgravity have been performed [1]. In this case, the gravity can be mostly neglected and we may observe various new aspects of dusty plasmas which have been hidden by the effect of gravity in experiments on earth. We may also expect the investigation of dusty plasmas under microgravity might lead to some new method to synthesize and process useful materials. The purpose of this paper is to extend our theoretical and numerical analyses on the structures of dusty plasmas under the gravity[2][3] and analyze dusty plasmas under microgravity.

We assume that the particles interact via the isotropic repulsive Yukawa potential

$$\frac{q^2}{r} \exp(-\kappa r), \quad (1)$$

where  $q$  is the charge and  $1/\kappa$  is the screening length. It is known that the ion flow in the sheath or other effects may induce anisotropy into the interaction. Here we show interesting features of the system without those effects, expecting that they remain so when the anisotropy is taken into account as a perturbation.

In the case of uniform one-component Yukawa system, we have two parameters, the density  $n$  and the temperature  $T$ , which we characterize by two dimensionless parameters

$$\Gamma = \frac{q^2}{k_B T a} \quad \text{and} \quad \xi = \kappa a, \quad (2)$$

where  $a$  is the mean distance defined by  $a = (3/4\pi n)^{1/3}$ .

In the case of mixtures with species  $i = 1, 2, \dots$ , we have the densities  $n_i$ , the charges  $q_i$ , the masses  $m_i$ , and the total number density  $n_{tot}$  as parameters:  $n_{tot} = \sum_i n_i$ . We here consider the case of binary mixtures and denote the species by  $i = 1, 2$ . We define the parameter  $\Gamma_1$  (denoted as  $\Gamma$  in figures) by

$$\Gamma_1 = \frac{q_1^2}{k_B T a}, \quad (3)$$

where the mean distance  $a$  is defined for the total density  $n_{tot}$  as  $a = (3/4\pi n_{tot})^{1/3}$ . In thermal equilibrium, static properties are characterized by the following four parameters

$$\Gamma_1, \quad \xi, \quad \frac{q_2}{q_1}, \quad \frac{n_2}{n_1}. \quad (4)$$

## EXTERNAL CONFINING POTENTIAL

We consider Yukawa systems in the environment of very small gravity and assume that Yukawa particles are spherically confined by an external potential. As the source of the external potential, we assume that the sheath with the uniform space charge

$$en_{sh} \quad (r > r_0) \quad (5)$$

surrounds the domain of electrically neutral plasma of radius  $r_0$ . We denote the electrostatic potential due to the charges in the sheath by  $\phi_{ext}(r)$ . The external potential for Yukawa particles with the charge  $-q$  is given by  $-q\phi$  or

$$-q\phi_{ext}(r) = 0 \quad (r < r_0) \quad (6)$$

and

$$-q\phi_{ext}(r) = \frac{q(4\pi en_{sh}r_0^3)/3}{r_0} \left[ \frac{1}{2} \left( \frac{r}{r_0} \right)^2 + \frac{r_0}{r} - \frac{3}{2} \right] \quad (r > r_0). \quad (7)$$

## NUMERICAL METHOD

In order to have as many particles as possible in the system, we here adopt the molecular dynamics with the  $O(N)$  scaling [5, 6]. The typical system size in our simulations is  $N = 10^4$ . The temperature is controlled by the Nosé-Hoover method. For mixtures, we assume the same mass for all species. In the classical case, the static properties do not depend on particles masses, though the relaxation time in general, especially for the energy, increases with the mass ratio: In this paper, we are interested in only static properties after relaxation.

## RESULTS AND DISCUSSION

### One-Component Yukawa System

Some examples of the results of simulations with  $10^4$  particles are shown in Figs. 1, 2, and 3, where the radial distributions and the position of shells are shown. The results are summarized as follows. (1) The system is separated into the outer and the inner parts. (2) In the outer part, a thin shell is formed at the surface of the system. The distribution of particles on this shell is a two-dimensional lattice with defects. Inside of the outermost shell, there appears a series of shells as in the case of one-component plasma confined by parabolic potential. The average density is higher than the inner part. (3) The shells become higher and sharper with the decrease of the temperature for fixed values of  $\xi$ . At fixed temperature, they become higher and sharper with the decrease of  $\xi$  or the increase of the coefficient of confining potential. (4) In the inner part, the average density is low and the shell structure is not clear.

### Yukawa Mixtures

The results for the mixture of Yukawa particles where the total number is  $10^4$  and  $n_2/n_1 = 1$ ,  $q_2/q_1 = 10$ , and  $q_2/q_1 = 5$  are shown in Figs. 4, 5 and 6. One of the most remarkable phenomena may be the separation of particles with different values of charges. This tendency becomes strong with the increase of the screening length and the decrease of the temperature. As for the relative position of shells of each species, we are still trying to give simple interpretations.

### Analysis of Structures at Low Temperatures in Fluid Limit

Here we present a theoretical analysis on the structure of one-component Yukawa particles at low temperatures based on the variational approach which is successful for the two-dimensional case [7]. In what follows we adopt the fluid approximation and express the density of particles by  $\rho(\mathbf{r})$ . The total number of particles  $N$  is related to  $\rho(\mathbf{r})$  by

$$\int d\mathbf{r} \rho(\mathbf{r}) = N. \quad (8)$$

The interaction is expressed as

$$U_{int} = \frac{q^2}{2} \iint d\mathbf{r} d\mathbf{r}' \frac{\exp(-\kappa|\mathbf{r} - \mathbf{r}'|)}{|\mathbf{r} - \mathbf{r}'|} \rho(\mathbf{r}) \rho(\mathbf{r}') \quad (9)$$

and the external potential is given by

$$U_{ext} = (-q) \int d\mathbf{r} \phi_{ext}(\mathbf{r}) \rho(\mathbf{r}). \quad (10)$$

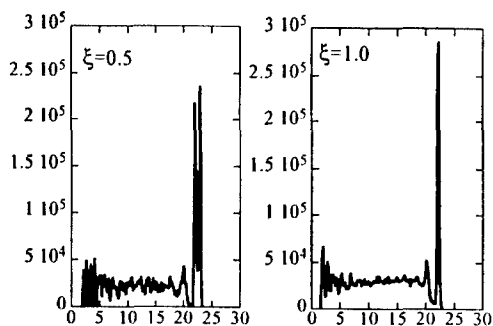


**FIGURE 1.** Distribution vs. radial distance measured in  $a$  in spherically confined Yukawa system under microgravity: Effect of screening length for  $\Gamma = 50$ .

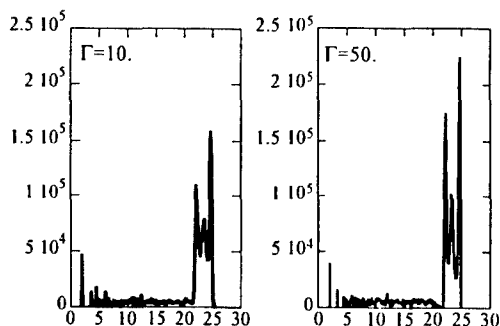


**FIGURE 2.** The same as Fig. 1: Effect of temperature for  $\xi = 0.1$ .

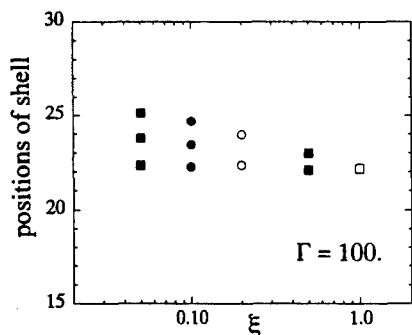


**FIGURE 3.** Position of shells measured in  $a$  vs.  $\xi$ .

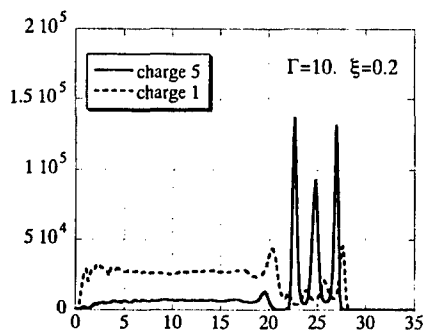


**FIGURE 4.** Distribution vs. radial distance measured in  $a$  in Yukawa mixture with charge ratio 5 ( $\Gamma = \Gamma_1$ ).

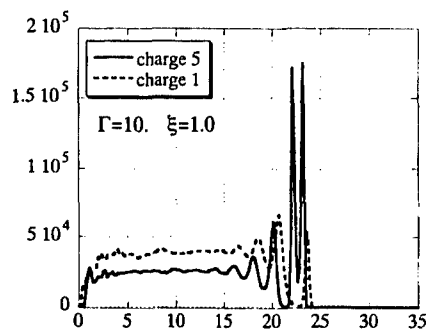


**FIGURE 5.** The same as Fig. 4 for  $\xi = 1.0$ .

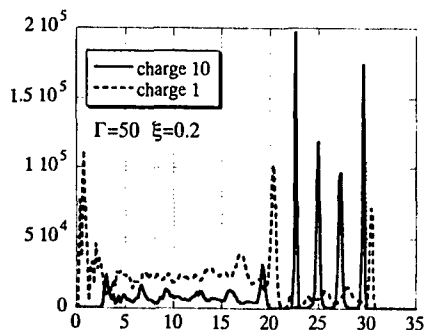


**FIGURE 6.** The same as Fig. 4 for charge ratio 10.

Let us find  $\rho(\mathbf{r})$  which minimizes the value of  $U_{int} + U_{ext}$  under the condition (8). The variation with respect to  $\rho(\mathbf{r})$  leads to

$$\int d\mathbf{r} \left[ (-q)\phi_{ext}(\mathbf{r}) + q^2 \int d\mathbf{r}' \rho(\mathbf{r}') \frac{\exp(-\kappa|\mathbf{r} - \mathbf{r}'|)}{|\mathbf{r} - \mathbf{r}'|} \right] \delta\rho(\mathbf{r}) = 0 \quad (11)$$

and

$$\int d\mathbf{r} \delta\rho(\mathbf{r}) = 0. \quad (12)$$

Denoting the Lagrange's multiplier by  $\mu$ , we have

$$(-q)\phi_{ext}(\mathbf{r}) + q^2 \int d\mathbf{r}' \rho(\mathbf{r}') \frac{\exp(-\kappa|\mathbf{r} - \mathbf{r}'|)}{|\mathbf{r} - \mathbf{r}'|} = \mu \quad (13)$$

and the value of  $\mu$  is determined by (8).

When we denote the source charge density of the external potential by  $e\rho_{ext}(r)$  as

$$\Delta\phi_{ext}(\mathbf{r}) = -4\pi e\rho_{ext}(\mathbf{r}), \quad (14)$$

we have from (13)

$$\rho(\mathbf{r}) = \frac{\kappa^2}{4\pi q} \phi_{ext}(\mathbf{r}) + \frac{e}{q} \rho_{ext}(\mathbf{r}) + \frac{\kappa^2}{4\pi q^2} \mu. \quad (15)$$

When the external charge density is given by (5), we have

$$\rho(r) = \frac{\kappa^2}{4\pi q^2} \mu \quad (r < r_0) \quad (16)$$

and

$$\rho(r) = \frac{\kappa^2}{4\pi q^2} \mu + \frac{e}{q} n_{sh} \left( 1 - \frac{1}{3} (\kappa r_0)^2 \left[ \frac{1}{2} \left( \frac{r}{r_0} \right)^2 + \frac{r_0}{r} - \frac{3}{2} \right] \right) \quad (r > r_0). \quad (17)$$

We observe that the density is low in the central part  $r < r_0$  and increases stepwise by  $(e/q)n_{sh}$  at  $r = r_0$ , separating the inner and outer parts of the system. This tendency is in agreement with the behavior of the results of simulation when the layering structure in the outer part is averaged: The latter seems to appear when the effect of discreteness or the correlation is taken into account.

When we denote the maximum radius of distribution by  $r_m$ , the condition (8) gives

$$\begin{aligned} \frac{N}{(4\pi r_0^3/3)} &= \frac{e}{q} n_{sh} \left[ \left( \frac{r_m}{r_0} \right)^3 - 1 \right] \\ &- \frac{e}{q} n_{sh} (\kappa r_0)^2 \left[ \frac{1}{10} \left( \frac{r_m}{r_0} \right)^5 - \frac{1}{2} \left( \frac{r_m}{r_0} \right)^3 + \frac{1}{2} \left( \frac{r_m}{r_0} \right)^2 - \frac{1}{10} \right] + \frac{\kappa^2}{4\pi q^2} \left( \frac{r_m}{r_0} \right)^3 \mu. \end{aligned} \quad (18)$$

This relation and the condition  $\rho(r_m) = 0$  determine the parameters  $\mu$  and  $r_m$ .

## Discussion

The average distribution may be understood within the consideration in the fluid limit and, since the repulsion between particles increases with the charge, we may naturally have the separation of charges in the case of mixtures. The formation of structures beyond the average distribution is related to the correlation between particles [2, 3].

It has been shown that particles distributed in the inner part may serve as the source of the force in the radial direction which plays the role of the gravity in the formation of layered structures [4]. The shells on the periphery in the one-component case thus correspond to the one-dimensional layers under the gravity. The structures in the case of mixtures seem to need more elaborate analysis.

## CONCLUSIONS

In this paper, we have analyzed the behavior of particles interacting via the repulsive isotropic Yukawa potential when the effect of gravity is neglected. In the confined Yukawa system of one species, the layered (shell) structure is formed from outer boundary of the system. This structure becomes clear and sharp with the decrease of the temperature or the increase of the screening length. Within each layer, particles are organized into two-dimensional lattice with defects.

When we have two kinds of Yukawa particles in our confined system, we have a separation according to the relative magnitude of charges: The species with larger charge tends to distribute on the periphery. There is also the tendency to form layered structures. Both becomes significant when the temperature is low and the screening length is large.

## ACKNOWLEDGMENTS

This work has been partly supported by the Grants-in-Aid for Scientific Researches from the Ministry of Education, Culture, Sports, Science, and Technology of Japan Nos. 08458109 and 11480110.

## REFERENCES

1. For example, G. E. Morfill *et al.*, Phys. Rev. Lett. **83**, 1598(1999).
2. H. Totsuji, T. Kishimoto, and C. Totsuji, Phys. Rev. Lett. **78**, 3113(1997).
3. H. Totsuji, T. Kishimoto, C. Totsuji, and T. Sasabe, Phys. Rev. E **58**, 7831(1998).
4. H. Totsuji, T. Kishimoto, C. Totsuji, and K. Tsuruta, Physica Scripta **T89**, 117(2001).
5. For example, S. Pfalzner and P. Gibbon, *Many-Body Tree Method in Physics*, Cambridge University Press, Cambridge, 1996;
6. L. Greengard and V. Rokhlin, J. Comp. Phys., **73**, 325(1987).
7. H. Totsuji, C. Totsuji, and K. Tsuruta, to appear in Phys. Rev. E.